



Minerva Access is the Institutional Repository of The University of Melbourne

**Author/s:**

Gunn, AP;Wong, BX;McLean, C;Fowler, C;Barnard, PJ;Duce, JA;Roberts, BR

**Title:**

Increased glutaminy cyclase activity in brains of Alzheimer's disease individuals

**Date:**

2021-03-01

**Citation:**

Gunn, A. P., Wong, B. X., McLean, C., Fowler, C., Barnard, P. J., Duce, J. A. & Roberts, B. R. (2021). Increased glutaminy cyclase activity in brains of Alzheimer's disease individuals. *Journal of Neurochemistry*, 156 (6), pp.979-987. <https://doi.org/10.1111/jnc.15114>.

**Persistent Link:**

<https://hdl.handle.net/11343/276032>

DR. ADAM PETER GUNN (Orcid ID : 0000-0002-8181-4975)

DR. PETER J BARNARD (Orcid ID : 0000-0003-1755-7991)

Article type : Original Article

## Increased glutaminyl cyclase activity in brain of Alzheimer's disease individuals

Adam P. Gunn<sup>1,2,#</sup>, Bruce X. Wong<sup>3</sup>, Catriona McLean<sup>4</sup>, Chris Fowler<sup>1</sup>, Peter J. Barnard<sup>5</sup>, James A. Duce<sup>1,3,\*</sup> and Blaine R. Roberts<sup>1,6,7,#,\*</sup> and The AIBL research group<sup>8</sup>

<sup>1</sup> Florey Institute of Neuroscience and Mental Health, The University of Melbourne, Parkville, Victoria 3010, Australia.

<sup>2</sup> Analytical Chemistry, Faculty of Science and Technology, University of Canberra, Canberra 2617, Australia.

<sup>3</sup> The ALBORADA Drug Discovery Institute, University of Cambridge, Cambridge Biomedical Campus, Hills Road, Cambridge, UK.

<sup>4</sup> Department of Anatomical Pathology, Alfred Hospital, Prahran, Victoria 3004, Australia.

<sup>5</sup> Department of Chemistry and Physics, La Trobe Institute for Molecular Science, La Trobe University, Victoria, 3086, Australia

<sup>6</sup> Department of Biochemistry, Emory School of Medicine, Atlanta, GA 30322 USA

<sup>7</sup> Department of Neurology, Emory School of Medicine, Atlanta, GA 30322 USA

<sup>8</sup> <http://www.aibl.csiro.au>

\* These authors had equal contribution

This is the author manuscript accepted for publication and has undergone full peer review but has not been through the copyediting, typesetting, pagination and proofreading process, which may lead to differences between this version and the [Version of Record](#). Please cite this article as [doi: 10.1111/JNC.15114](https://doi.org/10.1111/JNC.15114)

This article is protected by copyright. All rights reserved

## # Corresponding Authors:

Associate Professor Dr. Blaine Roberts, PhD

Emory School of Medicine

Department of Biochemistry

Department of Neurology

1510 Rollins Research Center

Atlanta, GA 30322 USA

Email: [blaine.roberts@emory.edu](mailto:blaine.roberts@emory.edu)

Dr. Adam Gunn, PhD

Analytical Chemistry

Faculty of Science and Technology

University of Canberra

Kirinari St, Bruce ACT 2617

E-mail: [adam.gunn@canberra.edu.au](mailto:adam.gunn@canberra.edu.au)**ABSTRACT**

Glutaminyl cyclases (QC) catalyze the formation of neurotoxic pGlu-modified amyloid- $\beta$  peptides found in the brains of people with Alzheimer's disease (AD). Reports of several-fold increases in soluble QC (sQC) expression in the brain and peripheral circulation of AD individuals has prompted the development of QC inhibitors as potential AD therapeutics. There is however a lack of standardized quantitative data on QC expression in human tissues, precluding inter-laboratory comparison and validation. We tested the hypothesis that QC is elevated in AD tissues by quantifying levels of sQC protein and activity in post-mortem brain tissues from AD and age-matched control individuals. We found a modest but statistically significant increase in sQC protein, which paralleled a similar increase in enzyme activity. In plasma samples sourced from the Australian Imaging, Biomarker and Lifestyle (AIBL) study we determined that QC activity was not different between the AD and control group, though a modest increase was observed in female AD individuals compared to controls. Plasma QC activity was further correlated with levels of circulating monocytes in AD individuals. These data provide quantitative evidence that alterations in QC expression are associated with AD pathology.

**KEYWORDS**

Glutaminyl Cyclase, Pyroglutamate, Alzheimer’s Disease, Amyloid- $\beta$ , Monocyte.

Word Count: 4733

## ABBREVIATIONS

AD, Alzheimer’s Disease

AIBL, Australian Imaging Biomarker and Lifestyle Study

AMC, 7-amino-4-methylcoumarin

APP, Amyloid Precursor Protein

A $\beta$ , Amyloid-beta peptide

CSF, cerebrospinal fluid

EDTA, ethylenediaminetetraacetic acid

isoQC, glutaminyl cyclase (Golgi-resident isoform)

MMSE, mini-mental state exam

NEM, N-ethylmaleimide

pGAP, pyroglutamate aminopeptidase

pGlu, pyroglutamate (5-oxoproline)

pGlu-A $\beta$ , pyroglutamate amyloid-beta peptide

QC, glutaminyl cyclase

sQC, soluble glutaminyl cyclase

TBS, Tris-buffered saline

## 1. BACKGROUND

A large body of *in vitro* and *in vivo* experimental evidence suggests A $\beta$  is a central contributor to neurodegeneration and cognitive dysfunction in AD [reviewed in (Murphy & LeVine 2010; Lista *et al.* 2015; Roberts *et al.* 2012)]. Cerebral A $\beta$  is not a discrete molecule, rather, it is represented by a family of amyloid peptides of differing lengths and post-translational modifications (Portelius *et al.* 2010; Piccini *et al.* 2005; Saido *et al.* 1995; Roher *et al.* 2017). Pyroglutamate-A $\beta$  (pGlu-A $\beta$ ) is one such modified A $\beta$  species, predominantly found in amyloid deposits of the AD brain (Saido *et al.* 1995; Mori *et al.* 1992; Piccini *et al.* 2005). Whilst pGlu-A $\beta$  peptides constitute a minor fraction of the total A $\beta$  in human brains (Portelius *et al.* 2010), they are resistant to aminopeptidase degradation, seed the formation of amyloid fibrils and show an increased propensity to damage neuronal membranes via pore

formation and lipid peroxidation (Gillman *et al.* 2014; Gunn *et al.* 2016; Schlenzig *et al.* 2012). Formation of pGlu-A $\beta$  is catalyzed by the enzyme glutaminyl cyclase (QC) (Cynis *et al.* 2008; Schilling *et al.* 2004) - pharmacological QC inhibition reduces pGlu-A $\beta$  levels and cerebral amyloid burden, improving cognitive function in transgenic AD mouse models (Schilling *et al.* 2008a; Schilling *et al.* 2008b; Wang *et al.* 2019). These findings, coupled with reports of elevated QC expression in AD tissues (Schilling *et al.* 2008b; Valenti *et al.* 2012; Morawski *et al.* 2014), have positioned QC as potential therapeutic target for AD.

QCs serve in various physiological roles by maturing peptide hormones, generating pGlu residues that form part of the functional ligand sequences in thyrotropin releasing hormone (TRH), gonadotropin releasing hormone (GnRH) and monocyte chemoattractant protein-1 (MCP-1/CCL2) (Abraham & Podell 1981; Fischer & Spiess 1987; Waniek *et al.* 2015; Hartlage-Rubsamen *et al.* 2015). The potential contribution of QC to AD pathology spurred the generation of libraries of QC inhibitor compounds (Buchholz *et al.* 2006; Wang *et al.* 2019; Li *et al.* 2017), though only one (PQ912) has thus far progressed to safety and tolerability testing in human clinical trials (Lues *et al.* 2015; Scheltens *et al.* 2018). Much recent interest in QC has centered around its association with AD, yet QC may also be a target for inflammatory disorders (Chen *et al.* 2012) and cancer immunotherapy (Logtenberg *et al.* 2019).

Two isoforms of QC are present in humans – a secreted form; soluble-QC (sQC), and a golgi-resident form; isoQC. The sQC and isoQC enzymes demonstrate similar substrate specificities *in vitro* (Stephan *et al.* 2009), though differences in cellular localization dictate their physiological substrates (Hartlage-Rubsamen *et al.* 2009; Cynis *et al.* 2008; Cynis *et al.* 2011). The generation of pGlu-A $\beta$  is thought to be due to sQC activity as the substrate amyloid precursor protein (APP) fragments and sQC colocalize in secretory granules (Hook *et al.* 2014; Hook *et al.* 2008). In the human brain, sQC is expressed primarily in neurons throughout the neocortex, hypothalamus, pituitary, hippocampus and subcortical nuclei (such as the Edinger-Westphal nucleus, locus coeruleus and nucleus basalis) (Morawski *et al.* 2010), and regulated by Ca<sup>2+</sup>-dependent transcription factors (De Kimpe *et al.* 2012). Across brain regions, laminar patterns of sQC expression are distributed between cortical layers (Morawski *et al.* 2010).

Only a handful of studies have looked at QC expression in the AD brain – one reported an increase in sQC protein in the temporal cortex determined by Western blot (Schilling *et al.* 2008b), while another found increased sQC immunoreactivity in distinct layers of the temporal and entorhinal cortices by histochemical staining (Morawski *et al.*

2014). In peripheral tissues, a relative increase in sQC protein expression was observed in monocytes of AD individuals compared to age-matched controls (Valenti *et al.* 2012), whereas CSF levels of QC activity were found to be the same in AD and control groups (Bridel *et al.* 2017). Increased cerebral levels of sQC mRNA have been reported in the temporal cortex (Schilling *et al.* 2008b; Morawski *et al.* 2014) and hippocampus (De Kimpe *et al.* 2012) of individuals with AD. While these studies have established evidence for a relative increase in sQC expression in AD tissues, standardized analyses of sQC protein or activity in the human brain are lacking. To evaluate sQC as a potential marker of AD pathology, we quantified the levels of sQC protein and activity in post-mortem human frontal cortex. We further compared levels of QC activity in plasma to determine if the enzyme activity has biomarker value in Alzheimer's disease.

## 2. METHODS

### 2.1. Chemicals & Reagents

The reaction substrates and standards 7-amino-4-methylcoumarin (AMC), glutamine-AMC (gln-AMC), pyroglutamate-AMC (pGlu-AMC) and alanine-AMC (ala-AMC) were purchased from Bachem (Bubendorf, Switzerland) and dissolved in DMSO. N-ethylmaleimide (NEM; Sigma Cat# E3876) was dissolved in 50% v/v ethanol and prepared fresh daily. Recombinant pfu pyroglutamate aminopeptidase (Cat# 7334) was purchased from Takara Biotechnology (Shiga, Japan). Unless stated all other reagents were purchased from Chem-Supply (Adelaide, Australia) and dissolved in ultrapure water (MilliQ, Millipore). PBD150 was synthesized as previously described (Buchholz *et al.* 2006).

### 2.2. Tissue Preparation

Human brain tissues used in this study were collected at autopsy; the sourcing and preparation of tissues was conducted by Victorian Brain Bank (VBB). AD pathological diagnosis and age-matched control designations were made by a qualified pathologist per National Institute on Aging – Reagan Institute criteria (Hyman *et al.* 2012); co-pathologies were excluded. All procedures were conducted in accordance with the Australian National Health & Medical Research Council's National Statement on Ethical Conduct in Human Research (2007), the Victorian Human Tissue Act 1982, the National Code of Ethical Autopsy Practice, and the Victorian Government Policies and Practices in Relation to Post-Mortem. Experiments were conducted under University of Melbourne human ethics

committee approval ID1136882 - informed consent was obtained for all human tissues used in this study.

Cortical tissues (100 – 200 mg) from Brodmann area 9 were homogenized by razor dissection in 5 volumes of tris-buffered saline (TBS; 10 mM Tris, 100 mM NaCl, pH 7.5) containing protease inhibitors (Complete, EDTA-free; Roche). The tissues were then sonicated (Branson Sonifer) for 3 rounds of 10 x 0.5 s bursts at 50% amplitude (0.5 s rest between bursts) with the tubes kept on ice. Tissue homogenates were centrifuged at 100,000 g for 20 min at 4 °C and supernatants (designated 'TBS soluble fraction') were added to fresh pre-chilled tubes and stored at -80 °C until required. Protein concentrations were determined by BCA assay (Pierce, Thermo Scientific) or a 2-D Quant kit (GE Healthcare Life Sciences).

Plasma samples were obtained from the Australian Imaging, Biomarker and Lifestyle Study of Ageing (AIBL; <https://aibl.csiro.au/about/>), collected in Li-Heparin tubes and stored as frozen aliquots at -80 °C. AD individuals included in the study were classified according to NINCDS-ADRDA (Alzheimer's Association) criteria. The recruitment and assessment process for AIBL subjects has been described elsewhere (Ellis *et al.* 2009). A sub-set of the AIBL cohort was used in the study, randomly selected with stratification for age-and-gender matching. Demographics of the donor brain and plasma samples are summarized in Table 1.

### 2.3. Immunoblotting

Western blotting was performed using standard protocols previously described (Gunn *et al.* 2016). Tissue extracts and recombinant protein standards were separated by SDS-PAGE using 4–12% XT Bis-Tris gels (Criterion, Bio-Rad) according to the manufacturer's instructions. Samples were transferred to pre-assembled nitrocellulose membrane stacks using a Trans-Blot® Turbo semi-dry transfer apparatus (Bio-Rad), applying 2.5 A for 7 min. Membranes were blocked using either 5% w/v non-fat dried milk or 2% bovine serum albumin (A3311, Sigma) dissolved in Tris-buffered saline (pH 8.0) containing 0.5% v/v Tween-20 (TBS-T). QC proteins were detected using rabbit polyclonal anti-QPCT (D01, Abnova) (RRID: AB\_10717329) (1:1000 in 5% milk TBS-T), mouse polyclonal anti-QPCT (A01, Abnova) (RRID: AB\_606897) (1:2000 in 2% BSA TBS-T) or rabbit polyclonal anti-QPCT (Abcam) (RRID: AB\_1925371) (1:1000 in 5% milk TBS-T). Primary antibody solutions were applied to membranes overnight at 4 °C. HRP-conjugated rabbit-anti-mouse or goat-anti-rabbit immunoglobulins (Dako) were applied to membranes at 1:10,000 dilution for 1 h at ambient temperature (nominally 23 °C). Membranes were washed four times (5 min each) with TBS-T after each antibody incubation step. Recombinant full-length (Cat#

H00025797-P01) and C-terminal (Cat# H00025797-Q01) GST tagged-sQC recombinant protein standards were purchased from Abnova. Protein loading was normalized by measuring total protein stained with Bio-Safe Coomassie as per the manufacturer's instructions (#1610786, Bio-Rad). Densitometry analyses were performed in Multigauge v3.0 (Fujifilm, Japan), using lane profiling to quantify target bands and background signals (polygonal line background). Western blotting was performed by a single analyst with samples labelled by an identifier number only (i.e. single blinded to sample grouping). Blinding was removed after the densitometry was performed to allow statistical analysis.

#### 2.4. QC Activity Analysis

Analysis of QC activity was performed by either fluorescence spectrometry adapted from published reports (Schilling *et al.* 2002; Schilling & Demuth 2004) or by a novel HPLC method developed here. For both the fluorescence spectrometry and HPLC methods the reaction mixture consisted of 50 mM Tris-HCl (pH 8.0), 0.1 mM glutamine-AMC (gln-AMC) and 0.2 mM N-ethylmaleimide (NEM). Reactions for fluorescence spectrometry additionally contained pyroglutamate aminopeptidase (pGAP) at 1 mU/mL (where 1 U = amount of enzyme that hydrolyses 1  $\mu$ mol of pGlu-p-nitroanilide per min at 37 °C, pH 7.0). To ensure the fluorescence assay specifically measured QC-catalyzed pGlu formation in our experimental conditions, different concentrations of frontal cortex extract and the reaction auxillary enzyme (pGAP) were tested in the presence or absence of the protease inhibitor N-ethylmaleimide (NEM) (data shown in supplementary material). The optimized conditions used to test the brain tissue cohort were 0.5 mg/mL cortical extract (protein level), 0.5 U/L pGAP and 0.2 mM NEM.

The HPLC method determines pyroglutamate-7-amino-4-methylcoumarin (pGlu-AMC) by absorbance at 324 nm following reversed-phase liquid chromatography (Fig. 1). Reactions for HPLC analysis were performed at 37 °C in 96 well microplates for 90 min and stopped by protein precipitation upon addition of 3 volumes of acetonitrile. Each plate was briefly shaken (30 s) before centrifugation (4000 g for 15 min at 4 °C) then supernatants transferred to a fresh microplate (#P-96-450V-C, Axygen Scientific) and dried by heated vacuum centrifugation (3 h at 40 °C). Dried reaction products were resuspended in 50  $\mu$ L of ultra-pure water containing 5  $\mu$ M alanine-AMC as an internal standard. Control reactions containing gln-AMC were used to subtract the level of non-enzymatic pGlu-AMC formation during incubation and sample handling. Chromatographic separation was performed using an Agilent XBD C18 (4.5  $\mu$ m x 50 mm) column by applying a gradient of acetonitrile

(containing 0.1 % v/v trifluoroacetic acid) (buffer B) against ultrapure water (MilliQ, containing 0.1 % v/v trifluoroacetic acid) (buffer A). A linear gradient of 10% - 25% v/v buffer B was applied over a 4.5 min period, then constant 25% buffer B for 0.5 min prior to re-equilibration at 10% buffer B. Flow rate was constant at 1.6 mL min<sup>-1</sup>. Peak integration of HPLC data were performed using OpenLAB CDS ChemStation (Agilent Technologies). Activity analyses were performed single-blinded using samples labelled with identifier number only (no grouping/diagnosis label) – blinding was removed after activity calculations were performed to allow statistical analysis.

## 2.5. Statistical Analyses

All data analyses were performed using Prism 8 (GraphPad Software). Statistical tests and sample sizes for each analysis are detailed in the figure legends. Normality was determined using D'Agostino and Pearson Test. Testing for outliers was performed using the ROUT method with Q = 1%; no outliers were identified or removed. Sample sizes for brain tissues were based on tissue availability. Sample sizes needed for the exploratory plasma study were determined by a power calculation (G\*Power software v3.1.9.3) using data from a pilot study of 10 control and 12 AD samples to estimate mean and standard deviation (group 1 = 0.517 ± 0.06, group 2 = 0.605 ± 0.122). The calculated effect size was then used to determine the required sample size (t-test; mean difference between two independent groups; a priori test to compute required sample size) using the following inputs: effect size = 1.046,  $\alpha$  = 0.05, two-tailed t-test, power = 0.95, allocation ratio = 1. The required sample size was calculated as 25 per group, 50 in total (critical t = 2.011). Analyses in this study were not pre-registered.

### 3. RESULTS

#### 3.1. sQC Protein and Activity Measurements in Human Brain

Previous studies of QC expression in human brain tissue have reported variable success when utilizing commercial antibodies (De Kimpe *et al.* 2012). We observed clear differences in the immunoblot profiles of brain tissues when probed with different commercially sourced QC antibodies. The D01 anti-sQC antibody (Abnova) detected bands at the approximate molecular weight of sQC in brain samples (approx. 38 kDa) but failed to recognize the recombinant sQC standard (Figs. 2A and supplementary material), thus precluding standardized quantitation of the immunoreactivities. A relative comparison of the D01 anti-sQC signals was instead performed for the cohort of AD and control brain extracts, revealing a significant elevation in the immunoreactive signals in the AD group (Fig. 2B). An alternative antibody, A01 anti-sQC (Abnova) produced two distinct bands at the approximate molecular weight of sQC in lanes containing human cortex while additionally detecting the recombinant sQC protein standard (Fig. 2C). The band corresponding to the approximate molecular weight of sQC (38 kDa) was used for densitometry analyses, despite the presence of multiple bands with either antibody. Comparatively, analysis of the same cohort with the A01 antibody and relating band densitometry to recombinant sQC standards identified a significant, though much smaller (1.24-fold) increase in mean sQC levels (Controls =  $22.35 \pm 4.0$ , AD =  $27.66 \pm 3.58$  ng/mg tissue) (Fig. 2D).

*Ex vivo* QC activity in these brain samples were also found to have a significant elevation in the AD group (Controls  $0.162 \pm 0.027$ , AD =  $0.191 \pm 0.032$  nmol min<sup>-1</sup> mg<sup>-1</sup>,  $p = 0.048$ ) (Fig. 3A), while specific activity was not different between groups (Fig. 3B). We further found a significant positive correlation ( $r^2 = 0.455$ ,  $p = 0.001$ ) between levels of sQC protein determined by Western blot and measured levels of enzyme activity (Fig. 3C), consistent with the Western specifically detecting the sQC protein.

#### 3.2. Comparison of QC Activity in Human Plasma

Following our observation that QC activity is altered in the AD brain, we investigated whether this difference was reflected in the peripheral circulation by comparing plasma samples from age and gender matched AD and control individuals. We were able to reliably measure QC activity in plasmas using a novel HPLC method. To validate the measurement of QC activity by this method we incubated human plasma samples in the presence of the PBD150 compound (Fig. 1C), a small molecule inhibitor of QC (Schilling *et al.* 2008b). These reactions demonstrated a large decrease in the peak corresponding to pGlu-AMC,

indicating that plasma QC activity was indeed inhibited by PBD150 and that this inhibition was detectable with the HPLC assay.

Mean levels of QC activity were not significantly different between AD and control groups (Fig 4A). Comparison of females within these groups (24 control females, 27 AD females) showed a modest increase in activity in AD females (12.3% mean increase, ANOVA  $p = 0.024$ ). Due to the subtle difference, the power of this result is considered preliminary and requires a larger validation study for confirmation (power analysis indicates a minimum of 59 individuals required per group to detect difference of 12% using  $\alpha = 0.05$ , power = 0.9). Levels of plasma QC activity were not found to correlate with mini mental state exam (MMSE) scores (Fig. 4B)

QC catalyzes the formation of pGlu (active) forms of thyrotropin releasing hormone (TRH) from its N-terminal glutamine precursor (Waniek *et al.* 2015), hence changes in QC expression may affect thyroid hormone signaling (Schilling *et al.* 2011). We therefore assessed whether plasma QC activities correlated with plasma thyroid stimulating hormone (TSH) and free-T3 (FT3), as well as the relationship between control and AD individuals. No significant correlations were observed between QC activity and either of these markers for the control or AD groups (supplementary material). A significant correlation was however observed in AD individuals between plasma QC activity and levels of circulating monocytes (Spearman correlation  $\rho = 0.285$ ,  $p = 0.049$ ) (Fig. 4C). This relationship was primarily driven by AD individuals with mild-moderate dementia (MMSE 13 – 24) – analysis of this sub-group demonstrated a stronger correlation (Spearman correlation  $\rho = 0.4873$ ,  $p = 0.005$ ) (Fig. 4D).

#### 4. DISCUSSION

Effective therapeutic interventions and non-invasive biomarkers for AD have remained elusive. Currently prescribed drugs offer modest symptomatic amelioration (Anand *et al.* 2017), while costly PET amyloid imaging, neurological testing and invasive CSF biomarker measurements are limited to a diagnosis of 'probable AD' ante-mortem. Immunotherapies targeting total amyloid have yielded little success to-date, though it is noteworthy that clinically-tested anti-A $\beta$  antibodies show fundamental differences in their capacity to bind amino-terminally modified A $\beta$  isoforms (Watt *et al.* 2014; Cynis *et al.* 2016), and may fail to engage abundant amino-truncated A $\beta$  isoforms in the AD brain such as pGlu-A $\beta$ . By contrast, rabbit polyclonal antibodies raised by vaccination with pGlu-A $\beta$  peptides were found to cross-react with full-length A $\beta$  isoforms (Perez-Garmendia *et al.*

2010). When these anti-pGlu-A $\beta$  antibodies were compared with a pan-A $\beta$  antibody in passive vaccination of transgenic mice, only the anti-pGlu-A $\beta$  antibody improved cognition even though both antibodies reduced plaque burden (Frost *et al.* 2015). Despite these promising pre-clinical results, translation of mouse immunotherapy studies to human trials presents many challenges [reviewed in (Cynis *et al.* 2016)]. Preventing the formation of pGlu-A $\beta$  peptides during the disease course is a novel and complementary alternative to amyloid clearing approaches such as passive anti-A $\beta$  vaccination. Cell culture and mouse studies have shown that significant pGlu-A $\beta$  formation is dependent on QC activity (Cynis *et al.* 2008; Cynis *et al.* 2006; Schilling *et al.* 2008a), hence there is opportunity to selectively target these isoforms independent of A $\beta$  synthesis via the APP proteolysis pathway.

While there has been significant recent interest in the role of pGlu-A $\beta$  and QC in AD pathology, only a small number of studies evaluating QC levels in human tissues are reported. Developing QC as a therapeutic target for AD will require further knowledge of QC expression in human health and disease. Technical limitations may in part account for the paucity of information on QC concentrations, with reported failures of commercial QC antibodies to specifically detect the target (De Kimpe *et al.* 2012). Our data confirm such differences, revealing vastly different band patterns by Western blot densitometry. With one antibody (D01), we demonstrated a several-fold increase in sQC levels in AD frontal cortex, which is similar to previous findings in the AD temporal cortex (Schilling *et al.* 2008b). Confidence in the accuracy of these relative quantifications is however limited, due to the absence of signal in several samples and uncertainty about the detection range and response per unit of QC (i.e. linear range and slope). Additionally, the D01 antibody failed to detect recombinant sQC standards, so the identity of the signal is not certain. By contrast, Western blots probed with the A01 antibody allowed us to compare signals in all samples against a standard curve of recombinant sQC, revealing a modest, though statistically significant increase in mean sQC levels in the AD frontal cortex. Other groups have likewise reported utility of the A01 antibody in producing the best signal-to-noise for the detection of sQC in human brain sections; immunohistochemistry studies employing the A01 antibody revealed elevated sQC protein in distinct cortical layers of the temporal cortex of AD individuals compared to age-matched controls (Morawski *et al.* 2014), concomitant with increased levels of sQC transcript. These data collectively suggest that sQC is increased in multiple regions of the AD brain due to heightened expression. The cause of this increase in brain QC expression is not yet known, though cell-culture studies have revealed that elevation of neuronal cytosolic calcium induces a several-fold increase in sQC expression (De Kimpe *et al.* 2012).

It is possible therefore that elevated levels of sQC are linked to changes in calcium signaling found in the AD brain [reviewed in (Agostini & Fasolato 2016)].

Our observations of increased sQC activity in the AD frontal cortex lend further support to the hypothesis that elevated sQC expression is a pathological feature of AD. This is consistent with a previous report describing a trend to increased QC activity in temporal cortex extracts of the AD brain compared to neurological controls (Morawski *et al.* 2014). Levels of QC activity in the plasma of AD individuals were not different to age-matched controls, indicating that QC expression is not altered *en masse* in AD. Peripheral changes in QC expression have previously been observed (Valenti *et al.* 2012) – sQC protein and mRNA were found to be elevated in peripheral blood monocytes of AD individuals compared to age-matched controls. Valenti *et al.* further found monocyte QC expression to correlate with decreased cognitive function (MMSE scores) and years of dementia. We observed a correlation between plasma QC activity and levels of monocytes in the peripheral blood of AD individuals, though we did not find a correlation between plasma QC activity and MMSE scores. It should be noted that the study by Valenti *et al.* utilized a cohort with a high proportion of females to males (approx. 2:1), and in our study a modest increase in plasma QC activity was limited to the female AD group. Collectively these results suggest that QC expression is altered in some individuals with AD and may be influenced by gender, though it is unlikely to serve as a diagnostic biomarker of AD in isolation. Yet, monitoring biofluid QC activity may have theragnostic value in clinical trials of QC inhibitors, as demonstrated in a recent phase 1 study of the QC inhibitor PQ912 (Lues *et al.* 2015).

QC activity is responsible for the conversion of monocyte chemotactic proteins (MCPs) to their bioactive pGlu-modified forms, and inhibition by the QC inhibitor PBD150 reduces monocyte migration (Chen *et al.* 2012). The contribution of QC activity to AD pathology may therefore be multi-faceted, driving cerebral pGlu-A $\beta$  production while additionally activating pro-inflammatory cytokines. Intriguingly, PBD150 reduces pGlu-A $\beta$  levels and total amyloid burden in the brains of transgenic AD mouse models (Schilling *et al.* 2008b), despite its reported inability to cross the murine blood-brain barrier (Brooks *et al.* 2015). QC inhibitors may therefore have multiple therapeutic benefits for AD that are independent of cerebral A $\beta$  activity. Clinical testing of QC inhibitors in AD has commenced, showing safety and tolerability in healthy individuals (Scheltens *et al.* 2018), with additional trials expected.

To our knowledge, we have reported here the first standardized quantitative comparisons of sQC protein in brain samples of control and AD individuals. Our analyses

provide further evidence that sQC levels are elevated in AD tissues and highlight the critical need to standardize measurements of QC expression.

--Human subjects --

Involves human subjects:

If yes: Informed consent & ethics approval achieved:

=> if yes, please ensure that the info "Informed consent was achieved for all subjects, and the experiments were approved by the local ethics committee." is included in the Methods.

ARRIVE guidelines have been followed:

No

=> if it is a Review or Editorial, skip complete sentence => if No, include a statement in the "Conflict of interest disclosure" section: "ARRIVE guidelines were not followed for the following reason:

Animals not used in study. Human ethics approval listed in manuscript. "

(edit phrasing to form a complete sentence as necessary).

=> if Yes, insert in the "Conflict of interest disclosure" section:

"All experiments were conducted in compliance with the ARRIVE guidelines." unless it is a Review or Editorial

## ACKNOWLEDGMENTS

APG would like to acknowledge project support and guidance from Ashley I. Bush and Robert A. Cherny (FINMH, University of Melbourne, Australia). We would like to acknowledge the volunteers and their families and the Australian Imaging and Biomarker, Lifestyle (AIBL) research team (<http://www.aible.csiro.au>). Tissues were received from the Victorian Brain Bank, supported by the University of Melbourne, Alfred Hospital, the Victorian Forensic Institute of Medicine and the National Health and Medical Research Council. We acknowledge funding from the Victorian Government's Operational Infrastructure Support Program. Partial support from the Australian Research Council Linkage Projects Scheme (with Agilent Technologies), the Cooperative Research Centre for Mental Health and the Alzheimer's Drug Discovery Research Foundation. BR is a National Health and Medical Research Council Dementia leadership fellow (grant ID APP1138673) and NHMRC project grant (ID: APP1164692). BR receives financial support from Agilent Technologies (Mulgrave, Victoria) and research support from Agilent technologies, Biosensis (Adelaide, South Australia) and eMSion (Corvallis, Oregon).

## COMPETING INTERESTS

James Duce is an editor for the Journal of Neurochemistry. The remaining authors do not declare any competing interests.

## REFERENCES

- Abraham, G. N. and Podell, D. N. (1981) Pyroglutamic acid. Non-metabolic formation, function in proteins and peptides, and characteristics of the enzymes effecting its removal. *Mol Cell Biochem* **38 Spec No**, 181-190.
- Agostini, M. and Fasolato, C. (2016) When, where and how? Focus on neuronal calcium dysfunctions in Alzheimer's Disease. *Cell Calcium* **60**, 289-298.
- Anand, A., Patience, A. A., Sharma, N. and Khurana, N. (2017) The present and future of pharmacotherapy of Alzheimer's disease: A comprehensive review. *Eur J Pharmacol*.
- Bridel, C., Hoffmann, T., Meyer, A., Durieux, S., Koel-Simmelink, M. A., Orth, M., Scheltens, P., Lues, I. and Teunissen, C. E. (2017) Glutaminyl cyclase activity correlates with levels of Abeta peptides and mediators of angiogenesis in cerebrospinal fluid of Alzheimer's disease patients. *Alzheimers Res Ther* **9**, 38.
- Brooks, A. F., Jackson, I. M., Shao, X., Kropog, G. W., Sherman, P., Quesada, C. A. and Scott, P. J. (2015) Synthesis and evaluation of [<sup>11</sup>C]PBD150, a radiolabeled glutaminyl cyclase inhibitor for the potential detection of Alzheimer's disease prior to amyloid beta aggregation. *Medchemcomm* **6**, 1065-1068.
- Buchholz, M., Heiser, U., Schilling, S., Niestroj, A. J., Zunkel, K. and Demuth, H. U. (2006) The first potent inhibitors for human glutaminyl cyclase: synthesis and structure-activity relationship. *J Med Chem* **49**, 664-677.
- Chen, Y. L., Huang, K. F., Kuo, W. C., Lo, Y. C., Lee, Y. M. and Wang, A. H. (2012) Inhibition of glutaminyl cyclase attenuates cell migration modulated by monocyte chemoattractant proteins. *Biochem J* **442**, 403-412.
- Cynis, H., Frost, J. L., Crehan, H. and Lemere, C. A. (2016) Immunotherapy targeting pyroglutamate-3 Abeta: prospects and challenges. *Mol Neurodegener* **11**, 48.
- Cynis, H., Hoffmann, T., Friedrich, D. et al. (2011) The isoenzyme of glutaminyl cyclase is an important regulator of monocyte infiltration under inflammatory conditions. *EMBO Mol Med* **3**, 545-558.

- Cynis, H., Scheel, E., Saido, T. C., Schilling, S. and Demuth, H. U. (2008) Amyloidogenic processing of amyloid precursor protein: evidence of a pivotal role of glutaminyl cyclase in generation of pyroglutamate-modified amyloid-beta. *Biochemistry* **47**, 7405-7413.
- Cynis, H., Schilling, S., Bodnar, M., Hoffmann, T., Heiser, U., Saido, T. C. and Demuth, H. U. (2006) Inhibition of glutaminyl cyclase alters pyroglutamate formation in mammalian cells. *Biochim Biophys Acta* **1764**, 1618-1625.
- De Kimpe, L., Bennis, A., Zwart, R., van Haastert, E. S., Hoozemans, J. J. and Scheper, W. (2012) Disturbed Ca<sup>2+</sup> homeostasis increases glutaminyl cyclase expression; connecting two early pathogenic events in Alzheimer's disease in vitro. *PLoS One* **7**, e44674.
- Ellis, K. A., Bush, A. I., Darby, D. et al. (2009) The Australian Imaging, Biomarkers and Lifestyle (AIBL) study of aging: methodology and baseline characteristics of 1112 individuals recruited for a longitudinal study of Alzheimer's disease. *Int Psychogeriatr* **21**, 672-687.
- Fischer, W. H. and Spiess, J. (1987) Identification of a mammalian glutaminyl cyclase converting glutaminyl into pyroglutamyl peptides. *Proc Natl Acad Sci U S A* **84**, 3628-3632.
- Frost, J. L., Liu, B., Rahfeld, J. U. et al. (2015) An anti-pyroglutamate-3 Abeta vaccine reduces plaques and improves cognition in APP<sup>swe</sup>/PS1<sup>DeltaE9</sup> mice. *Neurobiol Aging* **36**, 3187-3199.
- Gillman, A. L., Jang, H., Lee, J., Ramachandran, S., Kagan, B. L., Nussinov, R. and Teran Arce, F. (2014) Activity and Architecture of Pyroglutamate-Modified Amyloid-beta (A $\beta$ 3-42) Pores. *J Phys Chem B* **118**, 7335-7344.
- Gunn, A. P., Wong, B. X., Johanssen, T., Griffith, J. C., Masters, C. L., Bush, A. I., Barnham, K. J., Duce, J. A. and Cherny, R. A. (2016) Amyloid-beta Peptide A $\beta$ 3pE-42 Induces Lipid Peroxidation, Membrane Permeabilization, and Calcium Influx in Neurons. *J Biol Chem* **291**, 6134-6145.
- Hartlage-Rubsamen, M., Staffa, K., Waniek, A., Wermann, M., Hoffmann, T., Cynis, H., Schilling, S., Demuth, H. U. and Rossner, S. (2009) Developmental expression and subcellular localization of glutaminyl cyclase in mouse brain. *Int J Dev Neurosci* **27**, 825-835.
- Hartlage-Rubsamen, M., Waniek, A., Meissner, J. et al. (2015) Isoglutaminyl cyclase contributes to CCL2-driven neuroinflammation in Alzheimer's disease. *Acta Neuropathol* **129**, 565-583.
- Hook, G., Yu, J., Toneff, T., Kindy, M. and Hook, V. (2014) Brain pyroglutamate amyloid-beta is produced by cathepsin B and is reduced

- by the cysteine protease inhibitor E64d, representing a potential Alzheimer's disease therapeutic. *J Alzheimers Dis* **41**, 129-149.
- Hook, V., Schechter, I., Demuth, H. U. and Hook, G. (2008) Alternative pathways for production of beta-amyloid peptides of Alzheimer's disease. *Biol Chem*.
- Hyman, B. T., Phelps, C. H., Beach, T. G. et al. (2012) National Institute on Aging-Alzheimer's Association guidelines for the neuropathologic assessment of Alzheimer's disease. *Alzheimers Dement* **8**, 1-13.
- Li, M., Dong, Y., Yu, X. et al. (2017) Synthesis and Evaluation of Diphenyl Conjugated Imidazole Derivatives as Potential Glutaminyl Cyclase Inhibitors for Treatment of Alzheimer's Disease. *J Med Chem* **60**, 6664-6677.
- Lista, S., O'Bryant, S. E., Blennow, K., Dubois, B., Hugon, J., Zetterberg, H. and Hampel, H. (2015) Biomarkers in Sporadic and Familial Alzheimer's Disease. *J Alzheimers Dis* **47**, 291-317.
- Logtenberg, M. E. W., Jansen, J. H. M., Raaben, M. et al. (2019) Glutaminyl cyclase is an enzymatic modifier of the CD47- SIRPalpha axis and a target for cancer immunotherapy. *Nat Med* **25**, 612-619.
- Lues, I., Weber, F., Meyer, A. et al. (2015) A phase 1 study to evaluate the safety and pharmacokinetics of PQ912, a glutaminyl cyclase inhibitor, in healthy subjects. *Alzheimer's & Dementia: Translational Research & Clinical Interventions* **1**, 182-195.
- Morawski, M., Hartlage-Rubsamen, M., Jager, C. et al. (2010) Distinct glutaminyl cyclase expression in Edinger-Westphal nucleus, locus coeruleus and nucleus basalis Meynert contributes to pGlu-Abeta pathology in Alzheimer's disease. *Acta Neuropathol* **120**, 195-207.
- Morawski, M., Schilling, S., Kreuzberger, M. et al. (2014) Glutaminyl cyclase in human cortex: correlation with (pGlu)-amyloid-beta load and cognitive decline in Alzheimer's disease. *J Alzheimers Dis* **39**, 385-400.
- Mori, H., Takio, K., Ogawara, M. and Selkoe, D. J. (1992) Mass spectrometry of purified amyloid beta protein in Alzheimer's disease. *J Biol Chem* **267**, 17082-17086.
- Murphy, M. P. and LeVine, H., 3rd (2010) Alzheimer's disease and the amyloid-beta peptide. *J Alzheimers Dis* **19**, 311-323.
- Perez-Garmendia, R., Ibarra-Bracamontes, V., Vasilevko, V. et al. (2010) Anti-11[E]-pyroglutamate-modified amyloid beta antibodies cross-react with other pathological Abeta species: relevance for immunotherapy. *J Neuroimmunol* **229**, 248-255.

- Piccini, A., Russo, C., Gliozzi, A. et al. (2005) Beta amyloid is different in normal aging and in Alzheimer disease. *J Biol Chem* **280**, 34186-34192.
- Portelius, E., Bogdanovic, N., Gustavsson, M. K., Volkman, I., Brinkmalm, G., Zetterberg, H., Winblad, B. and Blennow, K. (2010) Mass spectrometric characterization of brain amyloid beta isoform signatures in familial and sporadic Alzheimer's disease. *Acta Neuropathol* **120**, 185-193.
- Roberts, B. R., Ryan, T. M., Bush, A. I., Masters, C. L. and Duce, J. A. (2012) The role of metallobiology and amyloid-beta peptides in Alzheimer's disease. *J Neurochem* **120 Suppl 1**, 149-166.
- Roher, A. E., Kokjohn, T. A., Clarke, S. G., Sierks, M. R., Maarouf, C. L., Serrano, G. E., Sabbagh, M. S. and Beach, T. G. (2017) APP/Abeta structural diversity and Alzheimer's disease pathogenesis. *Neurochem Int.*
- Saido, T. C., Iwatsubo, T., Mann, D. M., Shimada, H., Ihara, Y. and Kawashima, S. (1995) Dominant and differential deposition of distinct  $\beta$ -amyloid peptide species,  $A\beta_{N3(pE)}$ , in senile plaques. *Neuron* **14**, 457-466.
- Scheltens, P., Hallikainen, M., Grimmer, T. et al. (2018) Safety, tolerability and efficacy of the glutaminyl cyclase inhibitor PQ912 in Alzheimer's disease: results of a randomized, double-blind, placebo-controlled phase 2a study. *Alzheimers Res Ther* **10**, 107.
- Schilling, S., Appl, T., Hoffmann, T. et al. (2008a) Inhibition of glutaminyl cyclase prevents pGlu-Abeta formation after intracortical/hippocampal microinjection in vivo/in situ. *J Neurochem* **106**, 1225-1236.
- Schilling, S. and Demuth, H. U. (2004) Continuous assays of glutaminyl cyclase: from development to application. *Spectroscopy* **18**, 363-373.
- Schilling, S., Hoffmann, T., Manhart, S., Hoffmann, M. and Demuth, H. U. (2004) Glutaminyl cyclases unfold glutamyl cyclase activity under mild acid conditions. *FEBS Lett* **563**, 191-196.
- Schilling, S., Hoffmann, T., Wermann, M., Heiser, U., Wasternack, C. and Demuth, H. U. (2002) Continuous spectrometric assays for glutaminyl cyclase activity. *Anal Biochem* **303**, 49-56.
- Schilling, S., Kohlmann, S., Bauscher, C. et al. (2011) Glutaminyl cyclase knock-out mice exhibit slight hypothyroidism but no hypogonadism: implications for enzyme function and drug development. *J Biol Chem* **286**, 14199-14208.

- Schilling, S., Zeitschel, U., Hoffmann, T. et al. (2008b) Glutaminyl cyclase inhibition attenuates pyroglutamate Abeta and Alzheimer's disease-like pathology. *Nat Med* **14**, 1106-1111.
- Schlenzig, D., Ronicke, R., Cynis, H. et al. (2012) N-Terminal pyroglutamate formation of Abeta38 and Abeta40 enforces oligomer formation and potency to disrupt hippocampal long-term potentiation. *J Neurochem* **121**, 774-784.
- Stephan, A., Wermann, M., von Bohlen, A., Koch, B., Cynis, H., Demuth, H. U. and Schilling, S. (2009) Mammalian glutaminyl cyclases and their isoenzymes have identical enzymatic characteristics. *FEBS J* **276**, 6522-6536.
- Valenti, M. T., Bolognin, S., Zanatta, C., Donatelli, L., Innamorati, G., Pampanin, M., Zanusso, G., Zatta, P. and Carbonare, L. D. (2012) Increased Glutaminyl Cyclase Expression in Peripheral Blood of Alzheimer's Disease Patients. *J Alzheimers Dis.*
- Wang, X., Wang, L., Yu, X., Li, Y., Liu, Z., Zou, Y., Zheng, Y., He, Z. and Wu, H. (2019) Glutaminyl cyclase inhibitor exhibits anti-inflammatory effects in both AD and LPS-induced inflammatory model mice. *Int Immunopharmacol* **75**, 105770.
- Waniek, A., Hartlage-Rubsamen, M., Hofling, C., Kehlen, A., Schilling, S., Demuth, H. U. and Rossner, S. (2015) Identification of thyrotropin-releasing hormone as hippocampal glutaminyl cyclase substrate in neurons and reactive astrocytes. *Biochim Biophys Acta* **1852**, 146-155.
- Watt, A. D., Crespi, G. A., Down, R. A. et al. (2014) Do current therapeutic anti-Abeta antibodies for Alzheimer's disease engage the target? *Acta Neuropathol* **127**, 803-810.

## FIGURE LEGENDS:

**Figure 1. Measurement of QC activity by HPLC and fluorescence spectrometry. A)** Reaction schematic for fluorescence assays of QC activity (pGAP = pyroglutamate aminopeptidase; AMC = 7-amino-4-methylcoumarin). **B)** HPLC elution profile of the QC enzyme assay showing reaction substrate (gln-AMC, 1.9 min), internal standard (ala-AMC, 2.4 min), product (pGlu-AMC, 3.5 min) and cleaved product (AMC, 3.1 min) separated by reversed-phase HPLC with absorbance detection at 324 nm. **C)** Inhibition of plasma QC activity by PBD150 (100  $\mu$ M) demonstrates specificity in HPLC monitoring of pGlu-AMC formation (peak at 3.5 min).

**Figure 2: Western blot quantitation of sQC in human brain samples using different commercially sourced antibodies.** Extracts of human frontal cortical tissue extracts (20 µg/lane) and recombinant sQC protein standards were separated by SDS-PAGE and transferred to nitrocellulose (numbers left of blot represent approximate molecular mass in kDa). Comparison of relative sQC signals detected with the D01 antibody (Abnova) (A) and respective densitometry (B) (number of individual samples = 8 control and 8 AD). Representative blot of cortical tissue extracts and sQC protein standards probed with the A01 antibody (Abnova) (C) with quantitation of the full cohort measured in separate standardized blots shown in (D) (number of individual samples = 10 control and 9 AD). Only the lower band at ~38 kDa (approximate molecular mass of sQC) in each lane was used for densitometry quantification. All blots were normalized for protein loading by Coomassie staining of total protein. Boxes represent 25<sup>th</sup> to 75<sup>th</sup> percentiles with line at median; whiskers represent minimum to maximum data points. \* represents p-value < 0.05 (unpaired t-test with Welch's correction).

**Figure 3. Comparison of sQC protein expression and activity between control and AD brain tissues.** Levels of sQC activity (A) and specific activity (B) in control and AD frontal cortex extracts. Levels of sQC protein and activity were also correlated independent of disease (C). QC activity was determined by fluorescence spectrometry assay (number of individual samples = 10 control and 9 AD). Specific activity in (B) was calculated from activities shown in (A) and sQC protein determined using the A01 (Abnova) antibody on Western blots standardized with recombinant sQC. \* represents p-value < 0.05 (unpaired t-test).

**Figure 4. QC activities in human plasma from Alzheimer's disease (AD) and age-matched neurological controls from the AIBL cohort.** Plasma QC activities (A) were determined by HPLC assay (number of individual samples = 45 control, 47 AD), plotted against mini-mental state exam (MMSE) scores (B), and monocyte counts (C). Correlation between plasma QC activity and monocyte counts for AD individuals with mild-moderate dementia (MMSE 13 – 24) is shown in (D) (linear regression represented by solid line,  $r^2 = 0.2865$ ,  $p = 0.002$ ).

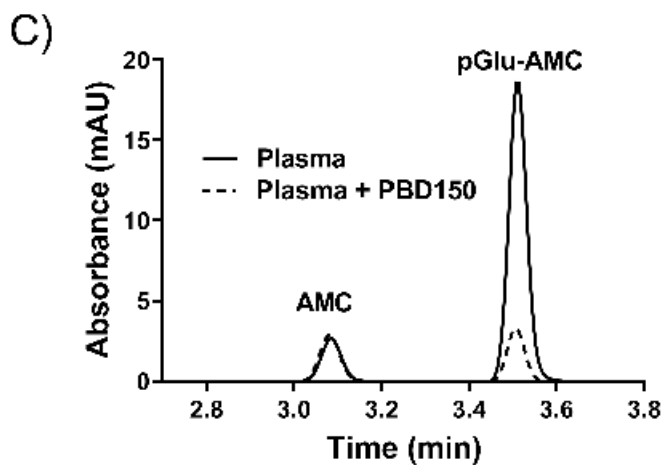
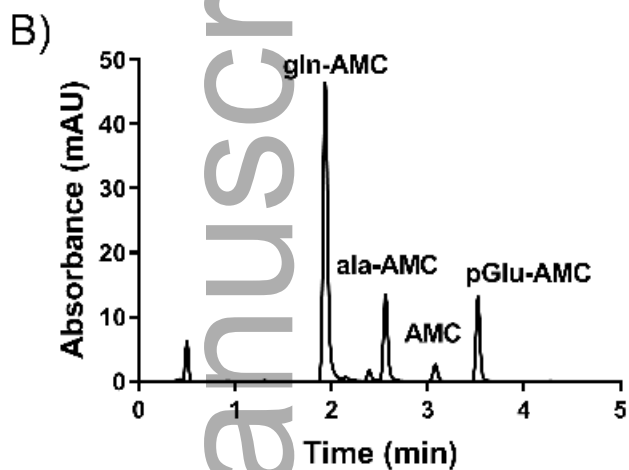
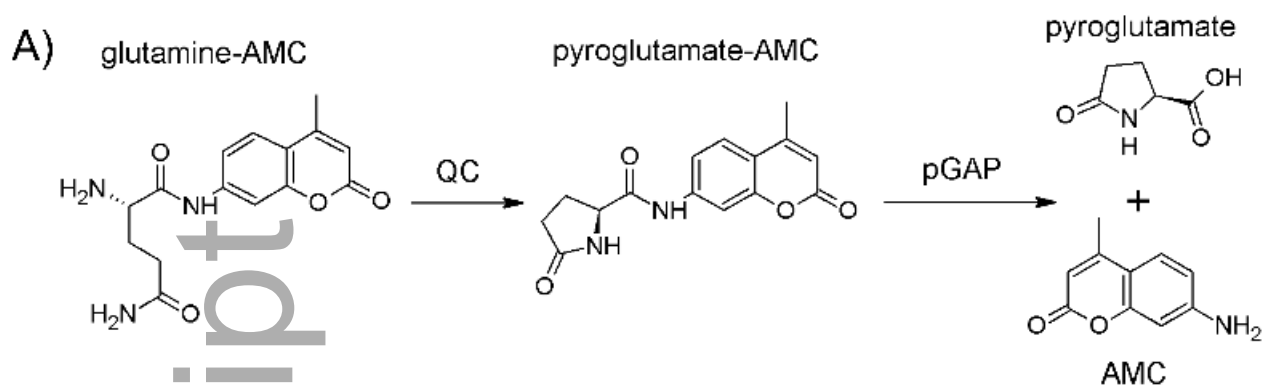
## Brain Samples

<b>Parameter</b>	<b>Control</b>	<b>AD</b>
Age (y) (mean $\pm$ s.d.)	60.5 $\pm$ 11.6	72.9 $\pm$ 14
Male / Female (total n)	8 / 2 (10)	6 / 3 (9)
PMI (h) (mean $\pm$ s.d.)	39.4 $\pm$ 16.4	45.7 $\pm$ 25.6

#### Plasma Samples

<b>Parameter</b>	<b>Control</b>	<b>AD</b>
Age (y) (mean $\pm$ s.d.)	74.2 $\pm$ 6.2	76.3 $\pm$ 8.4
Male / Female (total n)	21 / 24 (45)	21 / 26 (47)
MMSE (mean $\pm$ s.d.)	28.7 $\pm$ 1.2	16.4 $\pm$ 8.3

**Table 1:** Summary of donor tissue cohort demographics used in this study.



jnc\_15114\_f1.tif

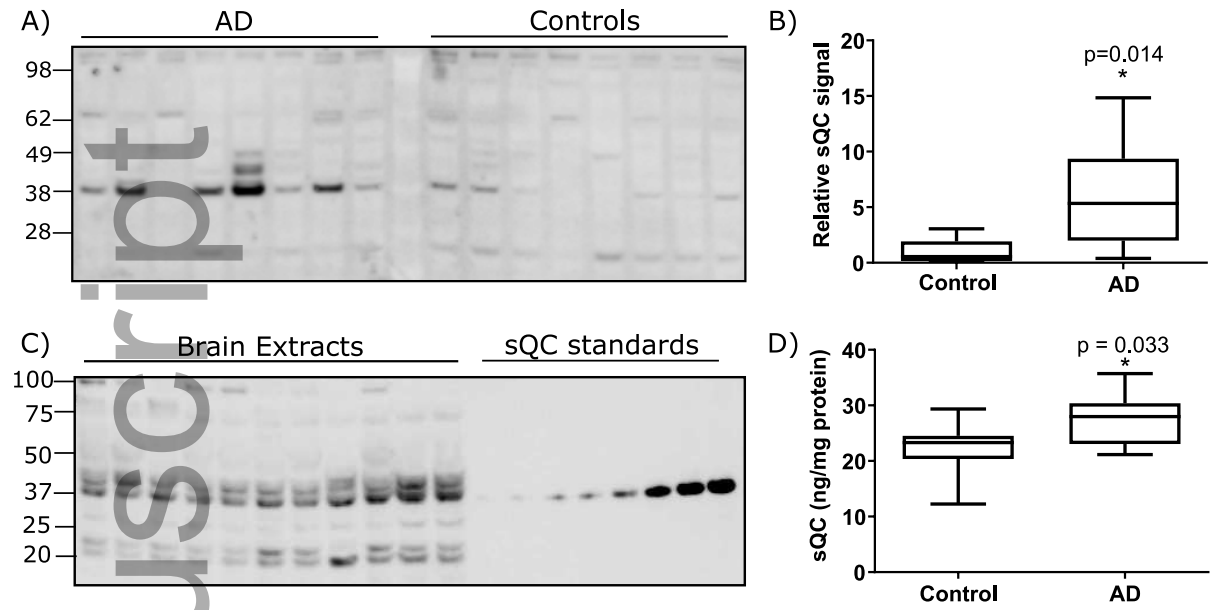
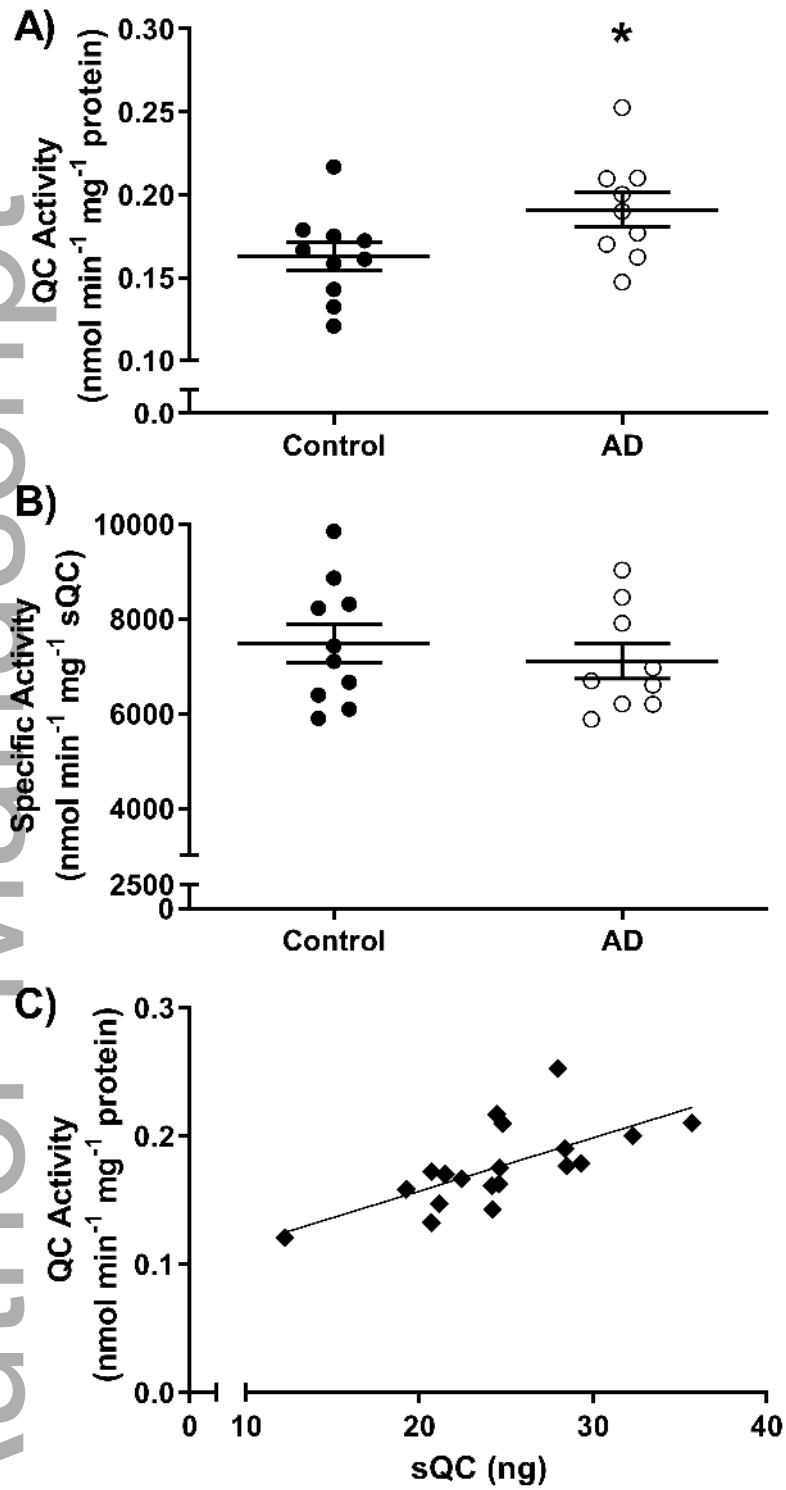
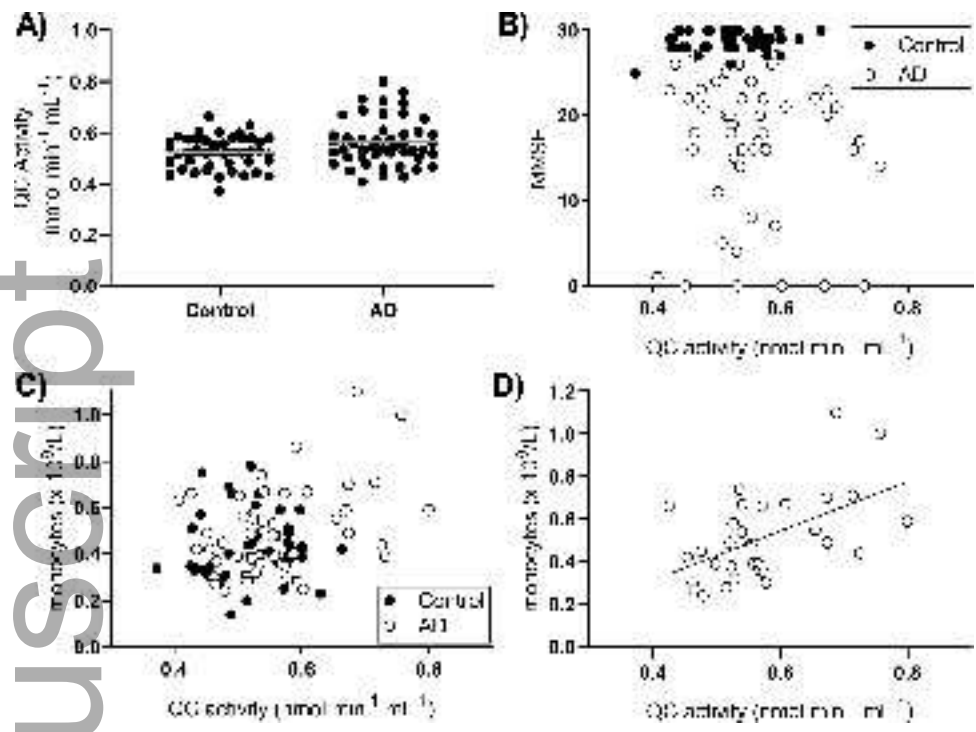


Figure 2.



jnc\_15114\_f3.tif



jnc\_15114\_f4.tif